J Biol Inorg Chem (2016) 21:851–863
DOI 10.1007/s00775-016-1384-5

ORIGINAL PAPER

Experimental and DFT characterization, antioxidant and anticancer activities of a Cu(II)–irbesartan complex: structure–antihypertensive activity relationships in Cu(II)–sartan complexes

María S. Islas[1] · Alicia Luengo[3,4] · Carlos A. Franca[1] · Mercedes Griera Merino[3,4] · Laura Calleros[3,4] · Manuel Rodriguez-Puyol[3,4] · Luis Lezama[2] · Evelina G. Ferrer[1] · Patricia A. M. Williams[1]

Received: 28 January 2016 / Accepted: 30 July 2016 / Published online: 9 August 2016

Abstract The coordination compound of the antihypertensive ligand irbesartan (irb) with copper(II) (CuIrb) was synthesized and characterized by FTIR, FT-Raman, UV–visible, reflectance and EPR spectroscopies. Experimental evidence allowed the implementation of structural and vibrational studies by theoretical calculations made in the light of the density functional theory (DFT). This compound was designed to induce structural modifications on the ligand. No antioxidant effects were displayed by both compounds, though CuIrb behaved as a weak 1,1-diphenyl-2-picrylhydrazyl radical ($DPPH^{\cdot}$) scavenger ($IC_{50} = 425\ \mu M$). The measurements of the contractile capacity on human mesangial cell lines showed that CuIrb improved the antihypertensive effects of the parent medication. In vitro cell growth inhibition against prostate cancer cell lines (LNCaP and DU 145) was measured for CuIrb, irbesartan and copper(II). These cell lines have been selected since the angiotensin II type 1 (AT1) receptor (that was blocked by the angiotensin receptor blockers, ARB) has been identified in them. The complex exerted anticancer behavior (at 100 μM) improving the activity of the ligand. Flow cytometry determinations were used to determine late apoptotic mechanisms of cell death.

Graphical Abstract Experimental and DFT characterization of an irbesartan copper(II) complex has been performed. The complex exhibits low scavenging activity against $DPPH^{\cdot}$ and significant growth inhibition of LNCaP and DU 145 prostate cancer cell lines. Flow cytometry determinations were used to determine late apoptotic mechanisms of cell death. This compound improved the antihypertensive effect of irbesartan. This effect was observed earlier for the mononuclear Cu–candesartan complex, but not in structurally modified sartans forming dinuclear or octanuclear Cu–sartan compounds.

Electronic supplementary material The online version of this article (doi:10.1007/s00775-016-1384-5) contains supplementary material, which is available to authorized users.

✉ Patricia A. M. Williams
williams@quimica.unlp.edu.ar

[1] Facultad de Ciencias Exactas, Centro de Química Inorgánica (CEQUINOR/CONICET/UNLP), Universidad Nacional de La Plata, Bv. 120 e/ 60 y 64 N°1465, 1900 La Plata, Argentina

[2] Departamento de Química Inorgánica, Facultad de Ciencia y Tecnología, Universidad del País Vasco, Apdo. 644, 48080 Bilbao, Spain

[3] Department of Systems Biology, Physiology Unity, Medicine School, University of Alcalá, Alcalá de Henares, Madrid, Spain

[4] IRSIN and REDinREN (Instituto de Salud Carlos III), Madrid, Spain

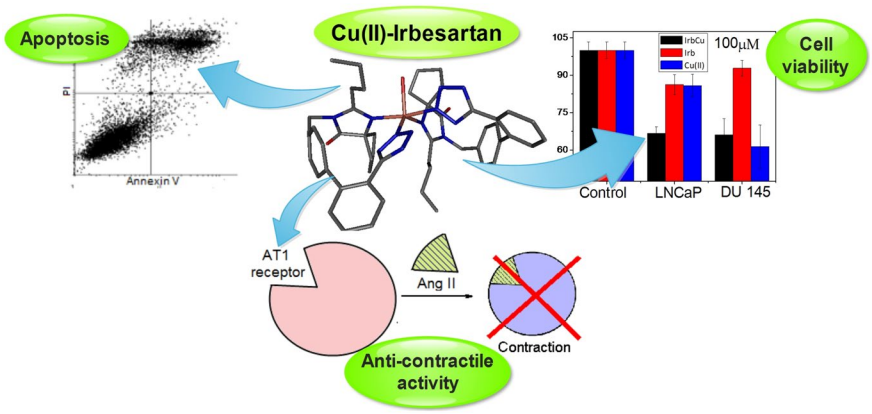

Keywords Irbesartan · Copper(II) complex · Antioxidant · Antihypertensive · Cytotoxicity

Abbreviations

ABTS	2,2′-Azino-bis(3-ethyl-benzothiazoline-6-sulfonic acid diammonium salt)
Ang II	Angiotensin II
ARBs	AT1 receptor blockers
AT1	Ang II type 1 receptor
CuIrb	$[Cu(Irb)_2(H_2O)]$, Irb: irbesartan
$DPPH^{\cdot}$	1,1-Diphenyl-2-picrylhydrazyl radical
DTA	Differential thermal analysis
HMC	Human mesangial cells
MTT	3-(4,5-Dimethylthiazol-2-yl)-2,5-diphenyltetrazolium bromide
NBT	Nitroblue tetrazolium
PBS	Phosphate buffered saline
PCSA	Planar cell surface area
PI	Propidium iodide
RAS	Renin–angiotensin system
SOD	Superoxide dismutase
TGA	Thermogravimetric analysis

Introduction

Angiotensin II (Ang II), the principal effector peptide of the renin–angiotensin system, plays a major role in the initiation and progression of vascular diseases, such as hypertension [1]. Angiotensin receptor blockers (ARBs) are well-tolerated drugs that are known to be useful for inhibiting activity of the renin–angiotensin system (RAS), treating hypertension and reducing the risk for cardiovascular disease.

The discovery and clinical use of first generation nonpeptide angiotensin II receptor antagonists represents a major success story in the history of cardiovascular medicine [2, 3]. These molecules were designed to block angiotensin II type 1 (AT1) receptors with the goal of reducing blood pressure and the risk for cardiovascular events. ARBs in use today are very well-tolerated antihypertensive drugs and are considered to offer protection against stroke, renal damage and cardiovascular disease [3]. This family of ARBs also called "sartans", are synthetic molecules with binding sites that at least partially overlap with Ang II binding site. These classes of molecules may approach the active site of the receptor by insertion in the lipid core, followed by lateral diffusion toward the binding site [4, 5]. Irbesartan (Fig. 1) is an ARB used mainly for the treatment of hypertension. It is a nonpeptide compound, chemically described as 2-butyl-3-[*p*-(*o*-1*H*-tetrazol-5-yl-phenyl)benzyl]-1,3-diazaspiro[4.4]non-1-en-4-one [6].

In addition to its role in the pathogenesis of hypertension, Ang II has been widely studied and identified to have growth factor and angiogenesis-promoting properties [7]. For this reason, AT1 receptor antagonists have been considered as potential tools in anticancer strategies [8]. There has been earlier evidence that AT2 blockade therapies suppress tumor growth, metastases, and angiogenesis in experimental animal models and reduce cancer prevalence in hypertensive patients [9].

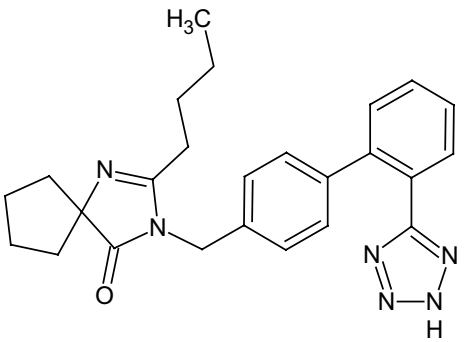

Fig. 1 Irbesartan structure

Metal complexes have been widely applied in clinics for centuries and the great successes achieved with platinum-based antitumor agents have promoted the development of metal-based drugs. Particularly, copper is an essential element involved in several biological functions. All tissues of the body need it for normal metabolic functions. Besides, the role of copper in maintaining cardiovascular health has been well established. Copper is essential both for its role in antioxidant enzymes, like Cu–Zn superoxide dismutase and ceruloplasmin, as well as its role in lysyl oxidase, essential for the strength and integrity of the heart and blood vessels. Copper deficiency has produced many of the same abnormalities present in cardiovascular disease [10]. Moreover, it has been demonstrated that the long-term use of hypotensive drugs may cause side effects, such as inverse disturbances in electrolyte homeostasis. The supplementation of these drugs with electrolytes such as zinc and copper increased the effectiveness of the treatment, and reduced the side effects of the hypotensive drugs [11].

Complexation of ARBs with some transition metals could be a useful strategy to develop novel antihypertensive drugs with enhanced properties such as antihypertensive, antioxidant and antitumoral. We have previously measured the effects of four analog copper(II) complexes with losartan [12], valsartan [13], candesartan [14] and telmisartan [15] and we have determined that upon complexation the antioxidant activities and the inhibitory effects on the tumoral cell line proliferation were improved. In this opportunity, we describe the preparation and structural characterization of a new copper(II) complex with irbesartan and determine its antioxidant behavior. The structural analysis of the complex has been determined by experimental and theoretical studies. Unfortunately, we could not obtain single crystals for X-ray structure analysis by dissolution of the solid using solvent mixtures at different ratios and evaporation, refluxing or by hydrothermal synthesis.

We have also determined the antihypertensive effect of the complex in comparison with the parent sartan measuring the inhibition of contraction induced by Ang II of both compounds and copper(II) on mesangial contractile cells and their antioxidant, cytotoxic properties and changes in cell cycle in prostate cancer cell lines. Particularly LNCaP and DU 145 cell lines were chosen since AT1 receptor has been identified in them [16].

Materials and methods

All chemicals were of analytical grade and used without further purification. Copper(II) chloride dihydrate was purchased from Riedel de Häen, pure commercial irbesartan (Hangzhou Garden Trading Co., Ltd (China)) was used as supplied. Elemental analyses (EA) for carbon, hydrogen and nitrogen were performed using a Carlo Erba EA 1108 analyzer. Thermogravimetric analysis (TGA) and differential thermal analysis (DTA) were performed with Shimadzu systems (models TG-50 and DTA-50, respectively), working in an oxygen flow of 50 mL min^{-1} and at a heating rate of 10 °C min^{-1}. Sample quantities ranged between 10 and 20 mg. Al_2O_3 was used as a differential thermal analysis standard. FTIR spectra of powdered samples (as pressed KBr pellets) were measured with an Equinox 55 FTIR-spectrophotometer from 4000 to 400 cm^{-1}. FT-Raman spectra were measured using the FRA 106 Raman accessory of a Bruker IFS 66 spectrophotometer. A continuous-wave Nd:YAG laser working at 1064 nm was employed for Raman excitation. Diffuse reflectance spectra were registered with a Shimadzu UV-300 instrument, using MgO as an internal standard. Electronic absorption spectra were recorded on a Hewlett-Packard 8453 diode-array spectrophotometer, using 1 cm quartz cells. A Bruker ESP300 spectrometer operating at the X-band and equipped with standard Oxford Instruments low-temperature devices (ESR900/ITC4) was used to record the EPR spectrum of the complex at room temperature in the solid state. A computer simulation of the EPR spectra was performed using the program SimFonia [17].

Synthesis of CuIrb

$[Cu(Irb)_2(H_2O)]$ (CuIrb): A solution of $CuCl_2{\cdot}2H_2O$ in ethanol (0.25 mmol, 3 mL) was added under continuous stirring to an ethanol solution of irbesartan (0.5 mmol, 10 mL). The obtained suspension was allowed to stir and was dissolved by the addition of an aqueous solution of 1 M NaOH. The final pH value was 6. A light green precipitate was observed and filtered off, washed several times with ethanol, and then dried in oven at 60 °C. Yield: 0.210 g, 85 %. Anal. Calc. %: C, 64.1; H, 5.9; N, 17.9. Exp. %: C, 64.0; H, 5.8; N, 17.8. Thermogravimetric analysis (TGA) confirmed the presence of one labile water molecule per copper atom (Exp. loss: 1.8 %. Calc. loss: 1.9 %; broad endothermic peak, 100 °C, DTA) (Figure S1). The water molecule is removed in the range 50–150 °C with a mass loss which corresponds to the calculated value. This temperature agrees with a probable labile $Cu–O_w$ bond due to the steric hindrance generated by the ligands. At 800 °C the weight loss (91.5 %, calc.; 91.6 %, exp.) represents the formation of CuO that was characterized by FTIR spectroscopy. UV–visible spectrum (DMSO): 750 nm broad (667 and 788 nm by deconvolution) (ε_{750} = 66.2 M^{-1} cm^{-1}). Diffuse reflectance spectrum: 398, 617 nm and 748 nm (deconvolution of the broad band).

Computational details

The stoichiometry of the complex, $[Cu(Irb)_2(H_2O)]$, has been determined taking into account the experimental assays considering the elemental analysis (two molecules of irbesartan per copper(II) atom), the presence of only one water molecule coordinated to the metal center (TGA-DTA), a coordination sphere consisting in 4 N as donor atoms (EPR) that interacted through the N sites of nitrogen moieties of the ligand (FTIR and Raman), see below. Computational methods were used to evaluate the stability of four different assumed structures by the employment of the density functional theory (DFT). The four starting structures of the complex were modelled as isolated molecules according to the experimental determinations. The optimization of the geometry for the four complexes were accomplished using the Truhlar M06-L [18] density functional with the LanL2DZ basis set which uses Dunning D95V basis set on all atoms [19]. Conducting polarizable continuous model (CPCM) calculations [20] were employed to simulate solvent effect in water. A vibrational analysis at the same level of theory was accomplished for the optimized complexes to verify whether they were local minima or saddle points on the molecular potential energy surface. The Raman activities (S_i) calculated by the GAUSSIAN-03 programs were converted to relative Raman intensities (I_i) using the following relationship [21]:

$$I_i = f(\nu_o - \nu_i)^4 S_i/\nu_i[-e(hc\nu_i)/kt],$$

where ν_o is the exciting wavenumber (in cm^{-1}); ν_i is the vibrational wavenumber of the *i*th normal mode; *h*, *c*, and *k* are the universal constants; and f is the suitably chosen common scaling factor for all the peak intensities. For simulation of Raman spectrum, pure Lorentzian line shapes were used with a bandwidth (FWHM) of 7 cm^{-1}.

Spectrophotometric titrations

The molar ratio method was used to establish the stoichiometry of the complexes in DMSO solution. The absorption spectra of different solutions of 0.05 M irbesartan with or without $CuCl_2{\cdot}2H_2O$ were measured. In both cases ligand-to-metal molar ratios from 8 to 1 were used and the pH values were adjusted to 6 with solid sodium methoxide, $NaOCH_3$.

Antioxidant properties

In these experiments irbesartan and the copper complex were dissolved in the minimum quantity of DMSO in order to avoid precipitations, and then they were added to the aqueous buffer and the substrate solutions. The same quantity of DMSO was added to the solutions for the basal state measurements in each case. The concentration of DMSO in each test was different but achieved a maximum of 2 % in the final reaction mixtures.

The antiradical activities of the compounds: scavenging power of the 1,1-diphenyl-2-picrylhydrazyl radical ($DPPH^{\cdot}$) radical, trolox equivalent antioxidant capacity (TEAC) measured by the 2,2′-azinobis(3-ethylbenzothiazoline-6-sulfonic acid) diammonium salt ($ABTS^{+\cdot}$) decoloration assay, inhibition of peroxyl radical and sequestering power of superoxide anion (determined by the superoxidedismutase (SOD) assay) were measured in triplicate according to previously reported methods [14]. Briefly, a methanolic solution of $DPPH^{\cdot}$ was added to the compound solutions in 0.1 M tris(hydroxymethyl)aminomethane-HCl buffer (pH 7.1) at 25 °C. The absorbance at 517 nm was measured after 60 min of the reaction in the dark and compared with the absorbance of control. For the decoloration of the $ABTS^{+\cdot}$ assay, this radical was generated by incubation of ABTS with potassium persulfate, and different concentrations of the compounds were added. These mixtures were incubated during 6 min at 25 °C. The trolox equivalent antioxidant capacity (TEAC) was calculated from the slope of the plot of the percentage inhibition of absorbance of $ABTS^{+\cdot}$, versus the concentration of the antioxidant divided by the slope of the plot for Trolox (6-hydroxy-2,5,7,8-tetramethylchroman-2-carboxylic acid). Peroxyl radicals have been generated by the thermal decomposition of 2,2-azobis(2-amidinopropane)dihydrochloride (AAPH). Pyranine (trisodium 8-hydroxypyerene-1,3,6-trisulfonate) was consumed by these radicals. The delay of pyranine consumption (lag phase) by peroxyl radicals in the presence of the competitive antioxidants was calculated as the time before the consumption of pyranine started (notable reductions in absorbance). The SOD activity was examined indirectly using the ability of the compounds to inhibit the reduction of nitroblue tetrazolium (NBT) by superoxide anion generated by the phenazine methosulfate (PMS) and NADH system.

Determination of changes in planar cell surface area (PCSA)

The human mesangial cells (HMC) were plated in 20-mm plates, and studies were performed before they reached confluence. Cells were pretreated with 10^{-8} M of the different compounds and after 15 min, 10^{-6} M Ang II was added. The cells were observed under phase contrast with an inverted PFX model TMS-F photomicroscope (magnification, 100×). Photographs of cells were taken at 0 min and after 30 min of Ang II addition. Every cell with a sharp margin suitable for the planimetric analysis was considered, and 6–12 cells were analyzed per photograph. PCSA was determined by computer-aided planimetric

techniques. Different controls were performed without the addition of irbesartan, CuIrb or Cu(II). The negative control was performed without Ang II addition, while in the positive control, Ang II was added. No contraction was observed in HMC due to treatment with compounds and without the addition of Ang II (data not shown).

Cell culture

The prostate cancer cell lines LNCaP (androgen-sensitive) and DU 145 (androgen-independent, derived from metastatic site: brain) were obtained from the American Type Culture Collection (ATCC, Manassas, VA, USA) and cultured in Roswell Park Memorial Institute (RPMI) 1640 medium supplemented with 100 U mL^{-1} penicillin, 100 μg mL^{-1} streptomycin and 7 or 10 % (v/v) fetal bovine serum (FBS) (Invitrogen, Prat de Llobregat, Barcelona, Spain), in the case of LNCaP and DU 145, respectively [22, 23].

Human mesangial cell lines (HMC) were cultured according to previously described procedures [22]. Portions of macroscopically normal cortical tissue were obtained from human kidneys immediately after a nephrectomy was performed because of renal cell carcinoma. Isolated glomeruli were treated with collagenase (Sigma) and plated on plastic culture dishes (Nunc, Kamstrup, Denmark). The identity of the cells was confirmed by previously described morphological and functional criteria [22]. When cells reached confluence, they were subcultured at a ratio of 1-4 in RPMI 1640 supplemented with 10 % fetal bovine serum (BioWhittaker, Walkersville, MD). Approval was granted by the Hospital Universitario Príncipe de Asturias Ethics Committee. The use of HMC was performed in accordance with the Declaration of Helsinki.

Cytotoxicity assays

The compounds were dissolved in DMSO just before each experiment and a calculated amount of these solutions was added to the cells achieving a final concentration of DMSO of 0.5 % which had no discernible effect on cell killing. For the metabolic activity of the prostate cancer cell lines determinations the cells were seeded into 24-well plates at a density of 2×10^4 per well. After 48 h, the medium was removed, the cells were washed with phosphate buffered saline (PBS) and cultured in RPMI 1640 with 10 % FBS containing the compounds to be studied at the appropriate concentration. Triplicate cultures were established for each treatment. After 24 h, the medium was removed and MTT (3-[4,5-dimethylthiazol-2-yl]-2,5-diphenyltetrazolium bromide) stock solution in PBS was added to the culture (final concentration 0.5 mg mL^{-1}) and the cells were incubated (2.5 h, 37 °C). Formazan crystals were dissolved in DMSO, and the absorbance has been measured on a microplate reader (test wavelength 570 nm, reference wavelength 690 nm) [24]. At least three independent experiments were performed for each experimental condition in all the biological assays. Results are expressed as mean ± SEM (standard error of the mean). Statistical differences were analyzed using ANOVA method followed by the test of LSD Fisher (least significant difference).

Flow cytometric analysis of apoptosis

Apoptosis was detected by Annexin V-FITC Apoptosis Detection Kit (BD Pharmingen™, BD Biosciences). Briefly, cells were collected after 24-h treatment with 100 μM concentration of the different compounds. Then, cells were double stained with annexin V-FITC and propidium iodide (PI) following manufacturer's instruction. Staining was measured by flow cytometry on a FACScan (Becton-Dickinson, BD Biosciences, San Agustín de Guadalix, Madrid, Spain) and the distribution of cells was analyzed using Cyflogic software. Data from 10,000 cells was collected for each data file.

Results and discussion

Vibrational spectra

In Table 1 and Fig. 2 the experimental vibrational FTIR and Raman spectra for irbesartan and CuIrb are shown. The assignments of the vibrational modes of the complex have been performed on the basis of the reported spectra of irbesartan using theoretical calculations [6] based on the density functional theory (DFT).

The disappearance of the N–H stretching band of irbesartan at 3426 cm^{-1} is indicative of the deprotonation and coordination of this group to the metal center. Furthermore, a stronger new band assigned to O–H stretching in the complex shows the presence of water. The bands in ca. 1700 cm^{-1} assigned to the C=O vibrations of irbesartan practically remained unaltered upon complexation. The main shifts due to coordination of the N atoms to copper(II) are observed in bands related to diazaspironone and tetrazole moieties. In the case of C=N stretching mode, the bands observed at 1619/1605 cm^{-1} (FTIR/Raman) for irbesartan, shifts to 1633/1610 cm^{-1} (FTIR/Raman) for CuIrb, a similar shift observed for other aromatic N containing ligands upon metal coordination [25–28]. Like in cyano complexes, on coordination to a metal the CN stretching shifted to higher frequencies, because the group acted as a σ-donor that tend to raise the frequency since electrons are removed from a weakly antibonding orbital. While the π backbonding of electrons from the metal to the ligand

Table 1 FTIR and Raman experimental frequencies and tentative assignments for irbesartan (Irb) and CuIrb complex

Tentative assignment	CuIrb		Irb[6]	
	FTIR	Raman	FTIR	Raman
ν NH ν OH	3455 (br, s)		3426 (br, m)	
ν C=O	1724 (vs)	1730 (w)	1733 (vs)	1730 (w)
ν C=N	1633 (vs)	1610 (vs)	1619 (vs)	1605 (vs)
δ $CNH_{ip\ arom}$	1511 (w)	1510 (m)	1512 (vw)	1516 (w)
δ NNH + ν CCH_{ip} + ν CN	1460 (s) 1434 (s)	1459 (s) 1426 (s)	1484 (m) 1462 w 1437 (s)	1490 (m)
δ NNH + ν CCH ip	1407 (sh) 1399 (s)		1409 (s)	1400 (s)
δ NNH + ν NN + ν $CC_{biphenyl\ bridge}$	1240 (w)		1238 (m)	1242 (s)
δ NNN + ν NN	1050 (vw)	1053 (m) 1006 (s)	1047 (m)	1053 (w) 1006 (w)
δ NNN	1013 (m) 1008 (m)		1018 (m) 1009 (m)	994 (w)

Wavenumbers are in cm^{-1} and relative experimental intensities

vs very strong, *s* strong, *m* medium, *w* weak, *vw* very weak, *br* broad, *sh* shoulder, *ν* stretching, *δ* bending, *arom* aromatic, *ip* in plane

tended to decrease the CN stretching, a better σ-donation prevailed and the CN stretchings were generally observed at higher energies upon complexation [29]. On the other hand, bands assigned to stretching and bending modes of tetrazole ring (NNN) change their position and/or intensity. Bands assigned to NNH bending modes shift or disappeared upon complexation, showing that the interaction to the metal center occurs through these functional groups.

The vibrational analysis of the characteristic bands of the complex was also performed by Raman spectroscopy (Fig. 2; Table 1). The band located at 1400 cm^{-1}, assigned to tetrazolic ring NNH twisting mode, disappeared in the Raman spectrum of the complex. Furthermore, two additional bands associated to tetrazolic ring, increased their Raman intensity in the complex. These bands, located in 1053 and 1006 cm^{-1} were assigned to NNN twisting and NN stretching modes. Then, the copper coordination via the nitrogen atoms of the tetrazolic and imidazole-like groups of irbesartan can be inferred by the observed changes in the individual Raman modes.

Electron spin resonance spectra

The X- band EPR powder spectrum of CuIrb was measured at 25 °C (Fig. 3). The spectrum showed a four-line hyperfine splitting pattern due to the coupling of the unpaired electron and the ^{63}Cu nucleus ($I = 3/2$).

The EPR signal showed a superhyperfine structure which can be attributed to the splitting produced by nitrogen nuclei in agreement with the presence of nitrogen atoms in the coordination sphere of metal center. From the EPR spectrum the Hamiltonian parameters $g_{//} = 2.270$ ($A_{//} = 170 \times 10^{-4}\ cm^{-1}$), $g_{\perp} = 2.059$ ($A_{\perp} = 17 \times 10^{-4}\ cm^{-1}$) and $A(4N) = 16.5 \times 10^{-4}\ cm^{-1}$ have been calculated. The simulated value of the parallel component of the hyperfine coupling constant is similar to that found in copper complexes with chromophores containing *N* donor atoms and the A^N parameter is indicative of the presence of four nitrogen donors quasi-equivalent situated at the corners of the equatorial plane around Cu(II) with a $d_{x^2-y^2}$ ground state [30]. Moreover, the values of $g_{//}$and $A_{//}$, the position of the electronic band in the visible region and the anisotropy of *g*-factors ($g_{//} > g_{\perp}$) presumes that an elongated square pyramidal chromophore CuN_4O is adopted [31].

A calculation of a *G* value ($G = (g_{//} - 2)/(g_{\perp} - 2)$) allowed the determination of the magnitude of the exchange interactions between the copper centers. A *G* value less than four indicates the presence of exchange interactions while a value higher than four is indicative of the absence of interaction [32]. In the CuIrb complex a *G* value of 4.58 has been calculated and then the interaction between the copper centers can be discarded.

Computational study and proposed structures for CuIrb

In agreement with the stoichiometry determined by experimental assays we have designed four possible structures for the CuIrb complex for the use of Molecular Modeling tools (Fig. 4).

This is the single possible arrangement given the different ways to join two irbesartan molecules coordinating by

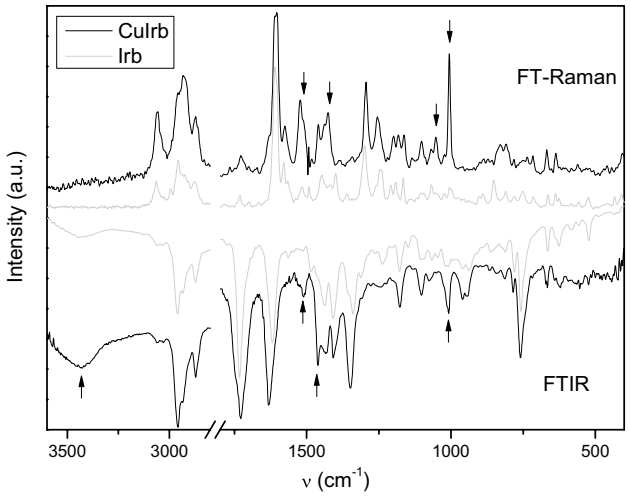

Fig. 2 Experimental FTIR and FT-Raman spectra of $[Cu(Irb)_2(H_2O)]$, CuIrb complex (*black*) and irbesartan, Irb (*gray*). The *arrows* indicate the main differences of the vibrational modes of both substances

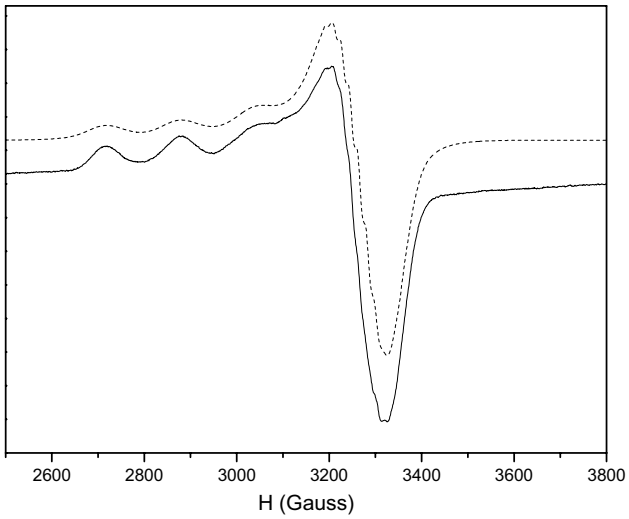

Fig. 3 EPR powder spectra (X-band) of the $[Cu(Irb)_2(H_2O)]$ (CuIrb) complex at 25 °C (*solid line*) and its simulated spectrum (WINEPR SimFonia) (*dotted line*)

the N-atoms and the only molecule of water with copper. In two of the isomers, the organic aliphatic chains of the ligand were oriented in the same direction (III and IV), and in the remaining two the aliphatic chains were oriented in opposite positions (I and II). For each case one coordinated water molecule was proposed. Due to the slight distortion in the vicinity of the copper atom the water positions above and below the equatorial plane are not equivalent. For this reason it was proposed to set the molecule of water above or below the plane for each pair of complexes (I, II and III, IV). We have performed the optimization of the geometry for complexes I–IV to obtain the structures of minimum energy. Theoretical vibrational spectra of all complexes were calculated to verify that they are all local minima. The electronic energy of each complex has been calculated and used to compare the relative stability between the four structures. A zero value has been assigned to the isomer with the lower calculated energy (Fig. 4, I) and increasing values, relative to zero, for the other three have been obtained. The second structure (Fig. 4, II) has almost the same energy value than complex I, with a value of only 0.003 kcal mol^{-1} above the former structure. The remaining two isomers showed energies of 3.1 kcal mol^{-1} (Fig. 4, III) and 4.4 kcal mol^{-1} above the most stable (Fig. 4, IV). The percentage contribution of each isomer was obtained using the Boltzmann Law Distribution at room temperature, showing near 50 % for the isomer I and a 50 % for the isomer II meanwhile the percentage of the two less stable isomers (III, IV) has been found near to zero. Therefore, a mixture of the two isomers I and II in a 1:1 ratio has been considered for the calculation of the theoretical vibrational spectra. Good concordance between the theoretical FTIR and Raman spectra and the experimental ones has been obtained (Fig. 5).

UV–Vis characterization in solution

The behavior of the complex in solution was studied using UV–Vis spectroscopy in order to determine the species present in solution and to compare it with the species formed in solid phase at the pH value of the preparative. The spectrophotometric titration of irbesartan:Cu (Fig. 6) was measured using different ligand-to-metal molar ratios in DMSO solutions at pH 6 adjusted with sodium methoxide, to prevent the formation of solid products due to the low solubility of the complex in water. A 2:1 (L:M) final stoichiometry was determined, in agreement with the structural determination of the solid complex.

Based on these data the visible spectrum of a 2:1 DMSO solution of irbesartan (0.05 M) and copper(II) (0.025 M) at different pH values has been measured (Fig. 7). It can be seen that the complex is formed in the pH range $4 < pH < 7$, with a broad band located at 750 nm, and the pattern agrees with the spectrum of the solid complex. At pH values above 7, a blue-shift of the band to 650 nm and solid precipitation can be observed.

The stability of the solid green complex in DMSO solution was also monitored by UV–Vis spectroscopy (from 0 to 90 min). The spectral changes showed that the absorbance of the band at 750 nm decreased in intensity ca. 3 % after 90 min (data not shown). Therefore, it can be seen that CuIrb is stable in DMSO solution at least during the preparation of the samples for the biological tests.

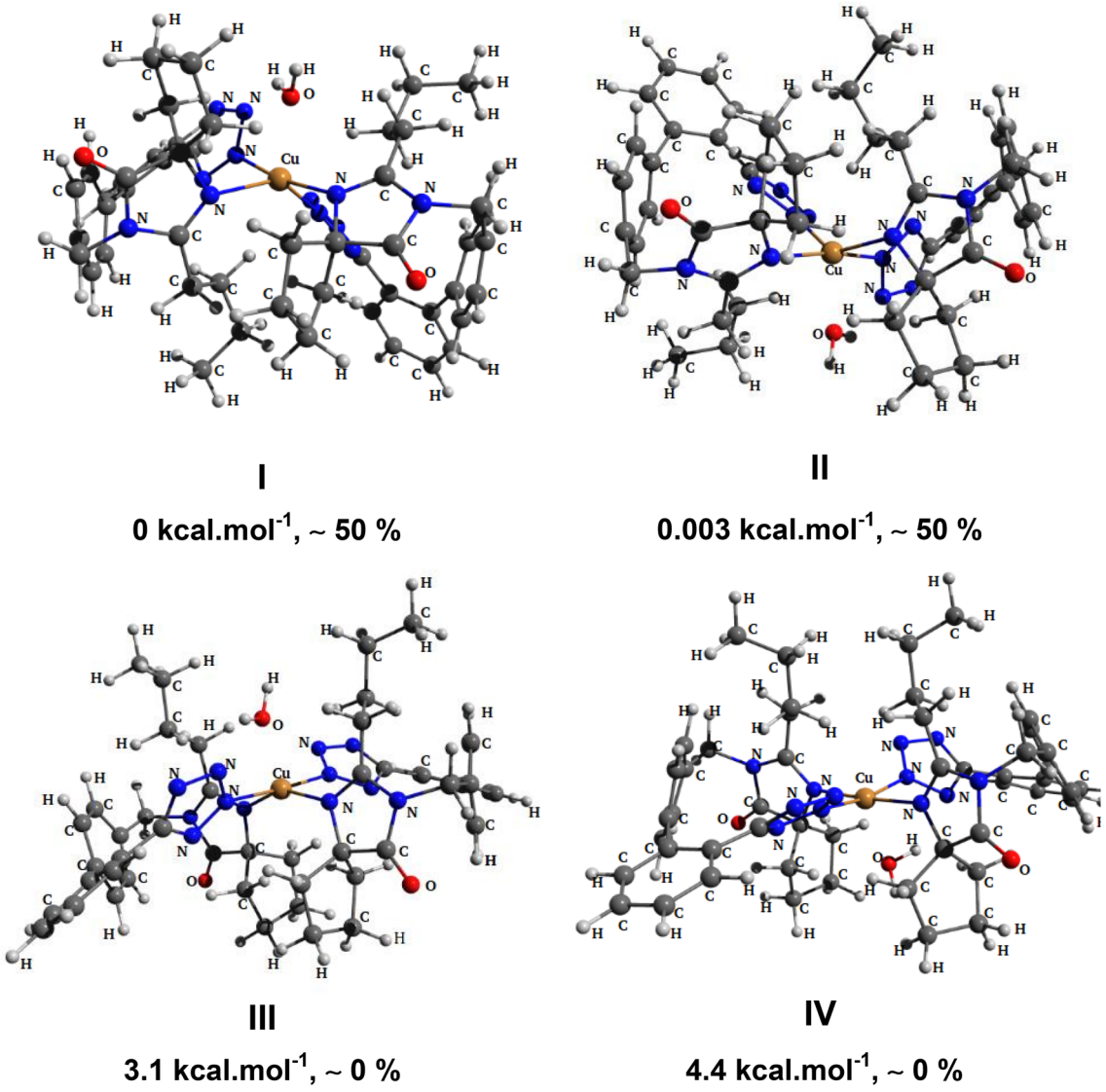

Fig. 4 Proposed structures for CuIrb complex isomers obtained by computational analysis, energy differences against most stable isomer (kcal mol^{-1}) and percent of contribution of each isomer according to Boltzmann distribution law

Antioxidant activity

The free radical scavenging capacities were measured on $DPPH^{\cdot}$, $ABTS^{\cdot+}$, peroxyl radicals, and superoxide anion. Irbesartan (Irb), CuIrb and $CuCl_2.2H_2O$ were tested in concentrations up to 500 μM. The obtained results showed that, while Irb and copper(II) salt were not able to scavenge any of these free radicals at the tested concentrations (data not shown), CuIrb exhibited a slight antioxidant activity solely against $DPPH^{\cdot}$ radicals (Fig. 8), showing statistically significant differences against the control and irbesartan in every tested concentration (from 50 to 500 μM). The IC_{50} value calculated for CuIrb was 425 μM, indicating the presence of a weak scavenger compound (IC_{50} value of ascorbic acid = 24.1 μM [33]).

No significant changes in the scavenging activity were observed for $ABTS^{\cdot+}$, peroxyl radicals, or superoxide anion for CuIrb at the tested concentrations. In a previous paper [34] it has been determined that irbesartan was able to scavenge $ABTS^{\cdot+}$ radicals, but the incubation period of the mixture of the different compounds and the radical was not reported.

It is a well known fact that oxidative stress is involved in the pathogenesis of several diseases and disorders. For this reason, the attention has focused on the role of antioxidants in the maintenance of human health, both in the prevention and treatment of diseases. We have previously measured the effects of the different sartans against free radicals. Our results show that they did not show antioxidant properties because of their very low scavenger power (see Table 2).

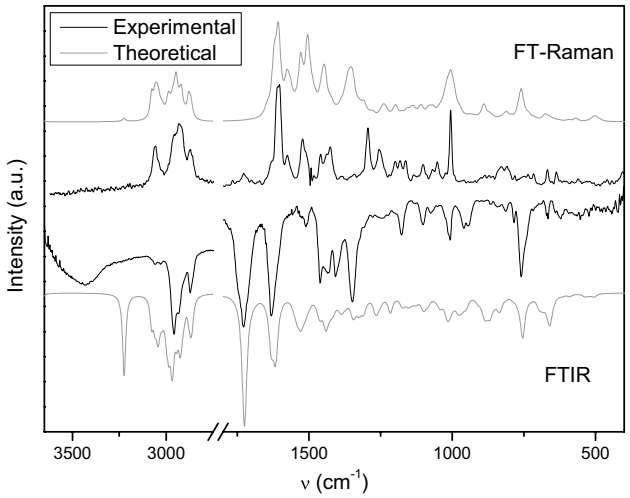

Fig. 5 FTIR and FT-Raman spectra of CuIrb complex. *Black* experimental, *gray* calculated

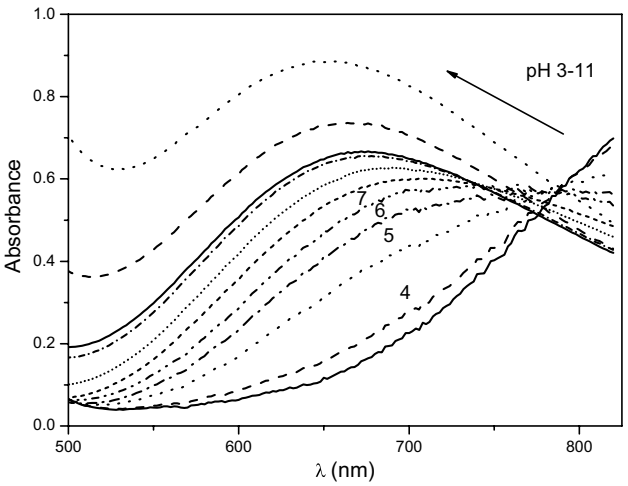

Fig. 7 Spectrophotometric determination of the formation of the CuIrb complex from copper(II) and irbesartan. Visible spectra of DMSO 2:1 solution of irbesartan (0.05 M) and $CuCl_2{\cdot}2H_2O$ (0.025 M) at different pH values from 3 to 11

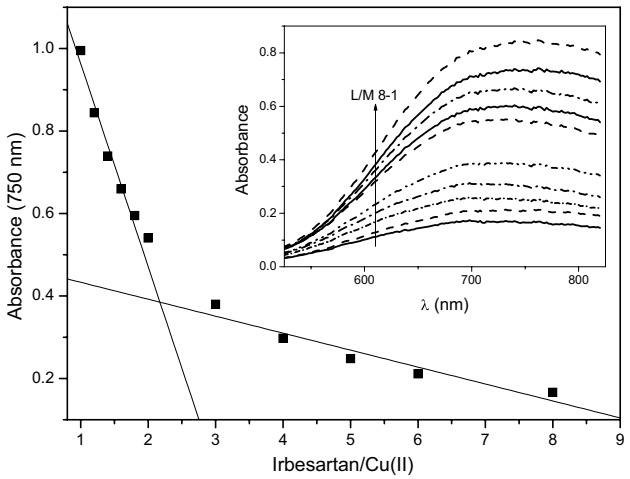

Fig. 6 Spectrophotometric determinations of CuIrb complex stoichiometry at 750 nm by the molar ratio method. *Inset* UV–Vis spectra of irbesartan (0.05 M) with the addition of $CuCl_2{\cdot}2H_2O$ in ligand-to-metal ratios (L/M) from 8 to 1 (pH 6, DMSO). The arrow indicates increasing metal additions

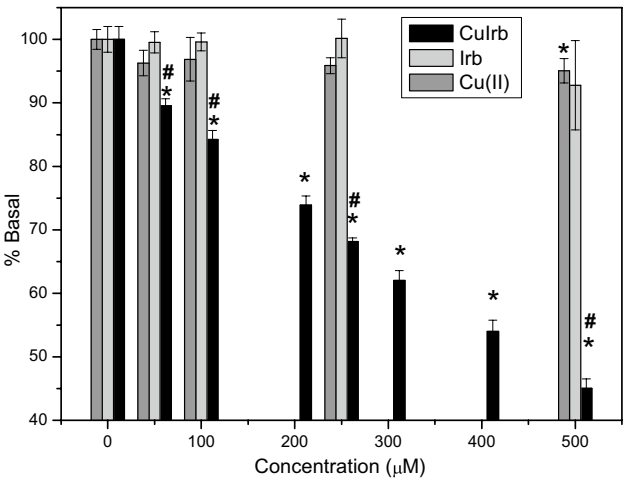

Fig. 8 Scavenging of 1,1-diphenyl-2-picrylhydrazyl radical ($DPPH^{\cdot}$) by irbesartan, CuIrb and $CuCl_2{\cdot}2H_2O$ (Cu(II)). The values are expressed as the mean ± standard error of at least three independent experiments. *Significant differences against control ($p < 0.05$). #Significant differences against ligand at the same concentration ($p < 0.05$)

This behavior has in general been improved by copper(II) complexation, at least against one of the tested radicals. The structural modification of the drug not only acts in the antihypertensive behavior (see below), but also the antioxidant effects against different radicals have been improved.

Contractile activity

Human mesangial cells express Ang II receptors and showed contractile response in the presence of this peptide as a consequence of its interaction with the receptor. The angiotensin receptor blockers (ARBs, sartans) are molecules of design that firmly bind to the receptor accounting for the antihypertensive efficacy. The antihypertensive effects have been tested by the analysis of the inhibition of the effect of Ang II to reduce the planar cell surface area (PCSA) in human mesangial cells (HMC) pretreated with irbesartan, CuIrb or Cu(II) salt (Fig. 9). The changes in PCSA are expressed as the percentage after 30 min incubation with Ang II, negative control has the 0 % value, whereas Ang II or the positive control has the highest contraction value ca. 19.3 %. For Cu(II) salts,

Table 2 Antioxidant tested properties of different sartans and their copper(II) coordination complexes

Compound	DPPH· (500 μM)	$ABTS^{\cdot+}$ (100 μM)	O_2^- (IC_{50}, μM)	ROO·
Los	ND	ND	ND	ND
CuLos[12]	ND	ND	72.5	ND
Cand[14]	94.05	95.08	>100	~0
CuCand[14]	93.27	92.72	5.5	~0
Tlm[15]	103.87	102.35	>100	~0
CuTlm[15]	79.57	101.68	7.2	~0
Irb	92.77	94.74	>100	~0
CuIrb	45.05	92.02	>100	~0

Los losartan, *Cand* candesartan, *Tlm* telmisartan, *Irb* irbesartan, *ND* non-determined

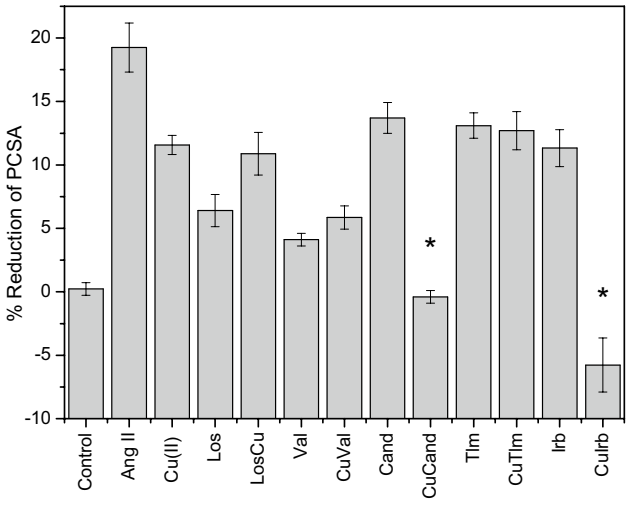

Fig. 9 Reduction percentage of the planar cell surface area (PCSA) (contraction induced by Ang II) in HMC cell line after incubation with 10^{-8} M of the different compounds and subsequent addition of 10^{-6} M Ang II. Control: cells without treatment. The mean ± SEM of three different experiments are shown. *Statistically significant differences of the action of the complexes with their parent free drugs ($p < 0.05$)

both copper(II) chloride and copper(II) acetate have been tested and similar results were obtained (11.6 and 10.9 %, respectively).

From Fig. 9 it can be seen that CuIrb produced an inhibitory action of the induced Ang II cell contraction, and that its action was statistically equivalent to that from the negative control (without Ang II), meanwhile copper(II) and irbesartan have showed a 11.6 and 11.4 % of reduction of PCSA, respectively, ca. 60 % of the positive control (treatment with Ang II). This result suggests that CuIrb might improve the antihypertensive activity of its parent drug irbesartan. Molecular docking has previously been used for a better understanding of how the sartans interacted with the receptor. From the predicted binding mode for irbesartan to the AT1 receptor binding pocket [35] it can be observed that the biphenyl moiety binds with different residues of the receptor. The N atoms of the tetrazole and the O atom of the 1,3-diazaspiro[4]non-1-en-4-one groups remain exposed outside the pocket. These functional groups acted as Lewis bases capable of sharing pair of electrons in forming coordinate bonds to copper(II) and therefore, CuIrb complex can bind the pocket in a similar manner than irbesartan. But complexation produces structural changes on the sartan. The presence of the two isomers I and II is postulated from the theoretical determinations of the structures of the complex calculated as isolated molecules with solvent effects (water). Upon dissolution the two isomers may accommodate in the pocket of the receptor in the same manner, not necessarily using the same geometrical structures than in the calculated isolated complex. Then, these structural differences could be responsible for a different occupation of the pocket improving the prevention of the agonist binding to a higher degree. All of these events may produce the desired effects of increasing the inhibition of the contraction induced by Ang II, which may lead to an improvement of the activity of irbesartan as antihypertensive drug.

Furthermore, the contractile capacity of Ang II in the HMC cells with previous incubation with LosCu and CuVal and their parent drugs were measured (Fig. 9) and these results have been compared with earlier determinations for CuCand [14] and CuTlm [15]. In two of the tested complexes (CuCand and CuIrb) we found a significant improvement with respect to the ligands. It is to be noted that these two complexes form mononuclear compounds while CuVal and LosCu are dinuclear complexes and CuTlm forms an octanuclear structure. Then, it can be suggested that the different structural modifications of the ARBs performed by complexation with the metal center could be the reason of the different occupation of the AT1 receptor with the concomitant competition of the binding of the pocket with Ang II. In particular, CuCand and CuIrb are supposed to block the receptor more efficiently than their parent sartans and then the subsequent addition of Ang II do not produce cellular contraction. Although each sartan differs in inducing inverse agonism with regard to its molecular interactions with the AT1 receptor, it has been shown that these molecules use their hydrophobic moieties to bind the receptor and such strong hydrophobic interactions are one of the important components to the higher affinity between them. As it has already been mentioned, the polar sites are exposed outside the receptor and these groups are capable of chelating metal ions. It can then be hypothesized that the mononuclear chelated complexes of sartans with copper(II) ion favored these

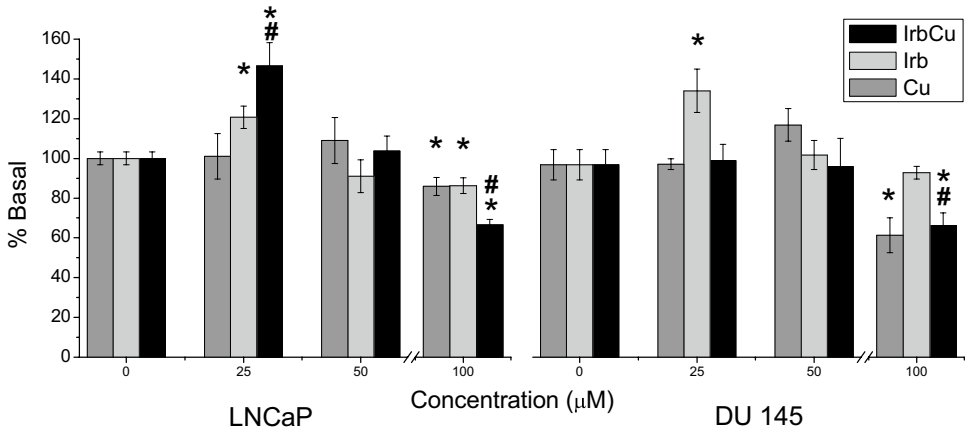

Fig. 10 Effects of copper(II), irbesartan (Irb), and their coordination complex (CuIrb) on the viability of LNCaP and DU 145 human prostate cancer cell lines determined by the MTT assay. Cells were incubated in RPMI with 10 % FBS (control) or with different concentrations of the compounds at 37 °C for 24 h. The results are expressed as the percentage of the basal level and represent the mean ± SEM ($n = 9$). *Significant differences versus basal $p < 0.05$. #Significant differences at the same concentration between CuIrb and Irb, $p < 0.05$

conformations and these structural changes could be assumed to be the cause of the higher capacity of CuCand and CuIrb to blocking the receptor.

Antitumor activity

It has previously been reported that irbesartan did not induce a reduction of cell viability and early apoptosis in prostate cancer cell lines and that telmisartan was the only tested ARBs that produce growth inhibition in these cell lines [36]. We have tested the effect of irbesartan, its copper complex, and the copper(II) salt $CuCl_2{\cdot}2H_2O$ on two different human prostate cancer cell lines: LNCaP and DU 145. Using the MTT assay (Fig. 10) it can be seen that CuIrb decreases significantly cell viability only at 100 μM, in the cell lines, while irbesartan only decreases it in LNCaP. At the highest concentration tested, CuIrb have shown to be a better antitumor compound than its parent drug, decreasing cell viability between 33 and 43 % from the basal. Copper(II), on the other hand, has shown antitumor activity at 100 μM as well, with a behavior in the DU 145 cell line similar to the complex but with smaller activity in the LNCaP cell line.

Mechanistic studies

With the aim of studying the mechanism of the decreasing in cell viability observed in the MTT assay, we have measured the induction of apoptosis in the two cell lines derived of prostate cancer by flow cytometry. Briefly, cells were treated with 100 μM copper(II), irbesartan or CuIrb for 24 h and then, double staining with Annexin V-FITC and propidium iodide (PI) were performed. In Fig. 11a dot plots divided into four quadrants are shown. The lower left quadrant (LL, Annexin V-FITC-/PI-) corresponds to live cell population, while upper left quadrant (UL, Annexin V-FITC−/PI+) corresponds to non-apoptotic necrotic cells; lower right quadrant (LR, Annexin V-FITC+/PI−) indicates early apoptotic cells and upper right quadrant (UR, Annexin V-FITC+/PI+) is indicative of cells undergoing secondary apoptosis and late stages of necrosis.

In the DU 145 cell line the copper complex has shown a slight but significant difference with control in late apoptosis population (UR) (Fig. 11b). On the other hand, in the LNCaP cell line, only slight differences in early apoptotic population (LR) were observed after treatment and, although no differences were found between irbesartan, copper(II) or CuIrb at 100 μM, an increasing of necrotic (UL) and late apoptotic (UR) population in all treatments in comparison with untreated control were observed.

Therefore, some correlations between antitumor activity measured by MTT assay and apoptosis assay performed with Annexin V-FITC and propidium iodide have been established. In both cell lines it can be seen that treatment with 100 μM CuIrb induced late apoptosis with a significantly decrease in cell surviving.

Conclusions

A new copper(II) complex with irbesartan $[Cu(Irb)_2(H_2O)]$ has been synthesized and characterized in solid phase and in DMSO solution. DFT studies were performed on CuIrb and both, vibrational assignment and simulated structure of four different isomers, were obtained. Antioxidant activity was measured against several radicals and CuIrb has only shown activity against $DPPH^{\cdot}$ radicals. The complex showed inhibition in cell viability in the tested human

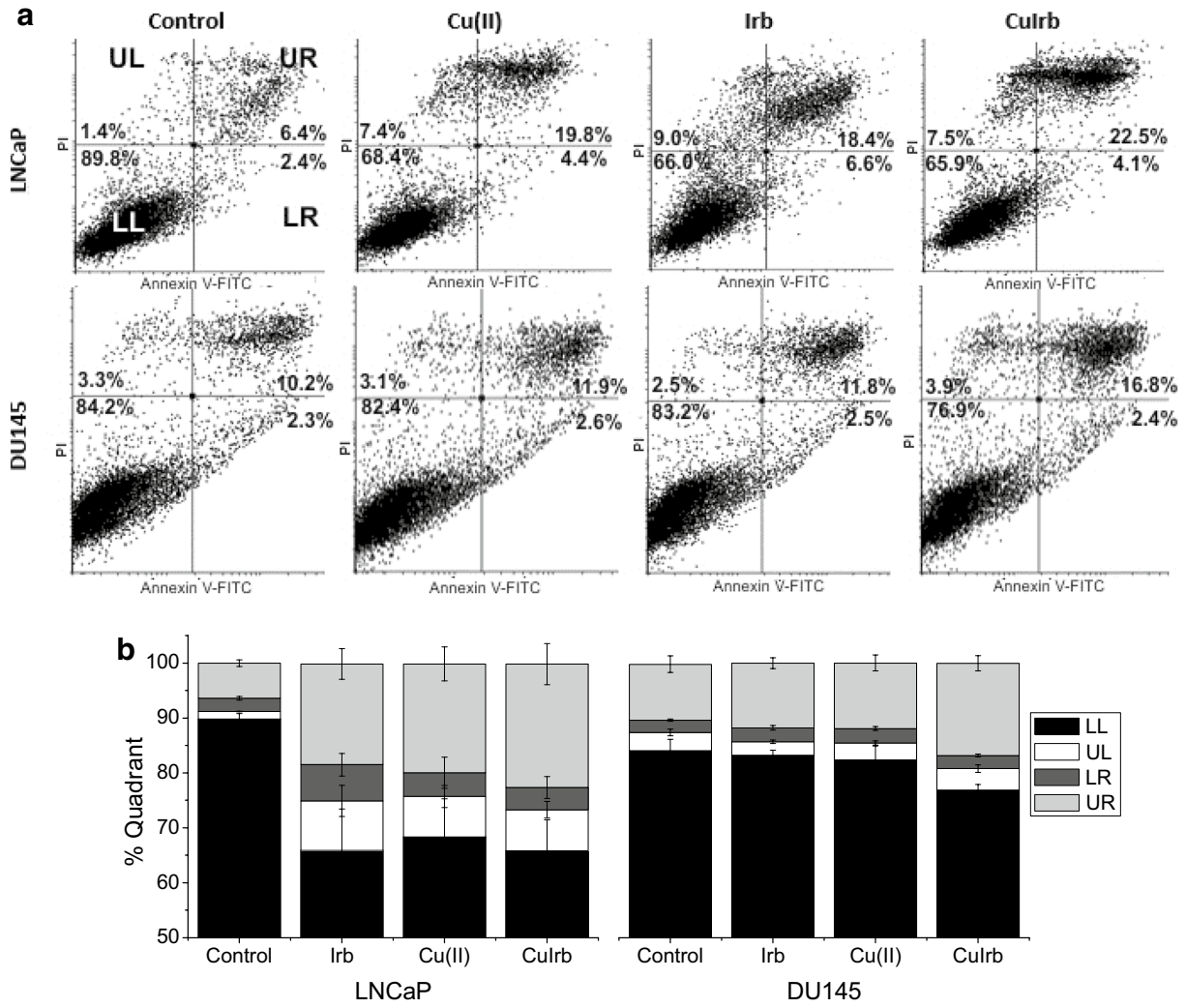

Fig. 11 **a** Dotplots of Annexin V-FITC vs. propidium iodide in the two cell lines derived from prostate cancer: LNCaP and DU 145 after treatment with 100 μM Cu(II), Irb or CuIrb for 24 h or for untreated cells (control). **b** Percentage of each quadrant vs. the different treatments. LL (in *black*), living cells; UL (in *white*), non-apoptotic necrotic cells; LR (in *dark gray*), early apoptotic cells; UR (in *light gray*), cells undergoing secondary apoptosis and late stages of necrosis. Data are expressed as a percentage of total cell number. Each *bar* represents the mean ± SEM of three different experiments performed in duplicate

prostate cancer cell lines at 100 μM in agreement with the increase in apoptotic cell population. On the other hand, CuIrb exhibits even higher efficiency as antihypertensive drug in comparison with the free medication expressing higher effect in the ability to block the Ang II action. A possible explanation of the correlation between structure and anti-contractile activity could be that the structural conformation of the complex is more similar to that of the pocket than the conformation that adopts irbesartan alone into the receptor. This new conformation could improve the interaction with the receptor, increasing by complexation the blocking ability of the irbesartan alone. Moreover, a structure–activity behavior could be established and a correlation between the antihypertensive capacity and the chemical structure of the copper–sartan complexes has been assessed.

Acknowledgments This work was supported by UNLP, CONICET (PIP 0611), CICPBA and by ANPCyT (PICT2013 0569), Argentina and Grant Renal Research Network: FEDER funds ISCIII RETIC REDINREN RD012/20021/0006, by Grant from Fondo de Investigaciones Sanitarias (FIS/ISCIII PI11/01630 and PI14/02075) to DRP and (FIS/ISCIII PI14/01939) to MRP integrated into the National Plan of I + D + i and co-funded by FEDER and the Instituto de Salud Carlos III and by Instituto de Investigaciones Sanitarias Reina Sofía (IRSIN) and Fundación Renal Iñigo Álvarez de Toledo (FRIAT). EGF and PAMW are research fellows of CONICET and CICPBA, Argentina, respectively. MSI is a fellowship holder from CONICET.

References

1. Garrido AM, Griendling KK (2009) Mol Cell Endocrinol 302:148–158
2. Duncia JV, Chiu AT, Carini DJ, Gregory GB, Johnson AL, Price WA, Wells GJ, Wong PC, Calabrese JC, Timmermans PB (1990) J Med Chem 33:1312–1329
3. Ram CVS (2008) Am J Med 121:656–663
4. Fotakis C, Christodouleas D, Zoumpoulakis P, Kritsi E, Benetis N-P, Mavromoustakos T, Reis H, Gili A, Papadopoulos MG, Zervou M (2011) J Phys Chem B 115:6180–6192
5. Potamitis C, Zervou M, Katsiaras V, Zoumpoulakis P, Kyrikou I, Argyropoulos D, Vatougia G, Mavromoustakos T (2009) J Chem Inform Model 49:726–739
6. Franca CA, Etcheverry SB, Diez RP, Williams PAM (2009) J Raman Spectrosc 2009:1296–1300
7. Abali H, Güllü IH, Engin H, Haznedaroğlu IC, Erman M, Tekuzman G (2002) Med Hypotheses 59:344–348
8. Deshayes F, Nahmias C (2005) Trends Endocrinol Metab 16:293–299
9. Arafat H, Gong Q, Chipitsyna G, Rizvi A, Saa CT, Yeo CJ (2007) J Am Coll Surg 204:996–1005 **(discussion 1005–1006)**
10. Klevay LM, Ann NY (1980) Acad Sci 355:140–151
11. Suliburska J, Bogdanski P, Jakubowski H (2014) Eur J Pharmacol 738:326–331
12. Etcheverry SB, Ferrer EG, Naso L, Barrio DA, Lezama L, Rojo T, Williams PAM (2007) Bioorg Med Chem 15:6418–6424
13. Etcheverry S, Di Virgilio AL, Nascimento OR, Williams PAM (2012) J Inorg Biochem 107:25–33
14. Islas MS, Lezama L, Griera Merino M, Cortes MA, Rodriguez Puyol M, Ferrer EG, Williams PAM (2013) J Inorg Biochem 123:23–33
15. Islas MS, Martínez Medina JJ, López Tévez LL, Rojo T, Lezama L, Griera Merino M, Calleros L, Cortes MA, Rodriguez Puyol M, Echeverría GA, Piro OE, Ferrer EG, Williams PAM (2014) Inorg Chem 53:5724–5737
16. Chow L, Rezmann L, Imamura K, Wang L, Catt K, Tikellis C, Louis WJ, Frauman AG, Louis SNS (2008) Prostate 68:651–660
17. Analytische Messtechnik-GmbH (1996) WINEPR SimFonia v1.25 software, Bruker
18. Zhao Y, Truhlar DG (2007) Theor Chem Acc 120:215–241
19. Dunning TH, Hay PJ (1977) In: Schaefer HF (ed) Methods of electronic structure theory, vol 3. Plenum press, New York
20. Casida ME, Jamorski C, Casida KC, Salahub DRJ (1998) Chem Phys 108:4439–4449
21. Keresztury G, Holly S, Besenyei G, Varga J, Wang A, Durig JR (1993) Spectrochim Acta Part A Mol Spectrosc 49:2007–2026
22. Cariaga-Martinez AE, López-Ruiz P, Nombela-Blanco MP, Motiño O, González-Corpas A, Rodriguez-Ubreva J, Lobo MVT, Cortés MA, Colás B (2013) Cell Signal 25:1586–1597
23. Luo C, Li Y, Zhou B, Yang L, Li H, Feng Z, Li Y, Long J, Liu J (2014) Apoptosis 19:542–553
24. Calleros L, Lasa M, Rodríguez-Álvarez F, Toro M, Chiloeches A (2006) Apoptosis 11:1161–1173
25. Williams PAM, Ferrer EG, Correa MJ, Baran EJ, Castellano EE, Piro OE (2004) J Chem Crystallogr 34:285–290
26. Dutta RL, Satapathi SK (1981) J Inorg Nucl Chem 43:1533–1539
27. Lane TJ, Nakagawa I, Walter JL, Kandathil AJ (1962) Inorg Chem 1:267–276
28. Klapötke TM, Schmid PC, Stierstorfer J, Szimhardt N (2016) Z Anorg Allg Chem 642:383–389
29. Nakamoto K (2009) Infrared and Raman spectra of inorganic and coordination compounds, Part B, 6th edn. John Wiley and Sons Inc, New Jersey
30. van Albada GA, Quiroz-Castro ME, Mutikainen I, Turpeinen U, Reedijk J (2000) Inorg Chim Acta 298:221–225
31. Tabbì G, Giuffrida A, Bonomo RP (2013) J Inorg Biochem 128:137–145
32. Hathaway BJ, Billing DE (1970) Coord Chem Rev 5:143–207
33. Yamaguchi T, Takamura H, Matoba T, Terao J (1998) Biosci Biotechnol Biochem 62:1201–1204
34. Wang M, Zhao X, Gai C, Liu H, Xu Y, Li J (2011) Chem Res Chinese Univ 27:1–5
35. Ohno K, Amano Y, Kakuta H, Niimi T, Takakura S, Orita M, Miyata K, Sakashita H, Takeuchi M, Komuro I, Higaki J, Horiuchi M, Kim-Mitsuyama S, Mori Y, Morishita R, Yamagishi S (2011) Biochem Biophys Res Commun 404:434–437
36. Funao K, Matsuyama M, Kawahito Y, Sano H, Chargui J, Touraine JL, Nakatani T, Yoshimura R (2008) Oncol Rep 20:295–300